

Intrinsic Magnetoresistance in Three-Dimensional Dirac Materials

Huan-Wen Wang, Bo Fu, and Shun-Qing Shen*

Department of Physics, The University of Hong Kong, Pokfulam Road, Hong Kong, China

(Dated: 24 March, 2018)

Recently, negative longitudinal and positive in-plane transverse magnetoresistance have been observed in most topological Dirac/Weyl semimetals, and some other topological materials. Here we present a quantum theory of intrinsic magnetoresistance for three-dimensional Dirac fermions at a finite and uniform magnetic field B . In a semiclassical regime, it is shown that the longitudinal magnetoresistance is negative and quadratic of a weak field B while the in-plane transverse magnetoresistance is positive and quadratic of B . The relative magnetoresistance is inversely quartic of the Fermi wave vector and only determined by the density of charge carriers, irrelevant to the external scatterings in the weak scattering limit. This intrinsic anisotropic magnetoresistance is measurable in systems with lower carrier density and high mobility. In the quantum oscillation regime a formula for the phase shift in Shubnikov-de Hass oscillation is present as a function of the mobility and the magnetic field, which is useful for experimental data analysis.

Introduction-Magnetoresistance is the value change of electric resistance of a material in an applied magnetic field, and depends on the mutual orientation of the electric current and the magnetic field. In a sufficient weak field, the origin of the magnetoresistance is highly related to the Lorentz force experienced by charge carries in the magnetic field and the spin-dependent scattering of electrons [1, 2]. Recently a positive in-plane transverse and negative longitudinal magnetoresistance have been observed in topological Dirac and Weyl semimetals[3–13], and some other metallic materials [14–17]. Especially the negative longitudinal magnetoresistance in Dirac and Weyl semimetals attracts great interests as its physical origin is possibly related to the chiral anomaly[18–20], a purely quantum mechanical effect, of the three-dimensional Weyl fermions in the electric and magnetic fields [21–25]. Several mechanisms without chiral anomaly are also proposed for conventional and topological metals [26, 27].

On the other hand, while the touching points of conduction and valence bands in the Weyl semimetals are protected topologically, the Dirac semimetals are located between conventional and topological insulators [28–30]. A small lattice distortion or external field can open a small energy gap in the band structure. Furthermore narrow gap semiconductors are also well described by the Kane model [31] in which the conduction and valence bands are strongly coupled together. A class of the gapless topological semimetals, and narrow-gap semiconductors or topological materials can be well described by an effective multi-band Dirac model [32–34]. In this class of materials, when the Fermi energy is located above the bottom of the conduction band, the transport properties are also affected by the existence of the valence bands as well as the conduction band. The strong band coupling in these materials produce prosperous physics of Berry phase in electron dynamics [35, 36].

In this Letter we propose an intrinsic origin of magnetoresistance of three-dimensional Dirac fermions in a finite magnetic field in the framework of the Kubo formula with the help of Landau levels. In the semiclassical regime, the quadratic corrections of a magnetic field are found to both longitudinal and in-plane transverse resistivity and the electrical mobility.

As a consequence the relative magnetoresistivity is quartic of the ratio of the Fermi wave length (the reciprocal of the Fermi wave vector) to the magnetic length. In the weak scattering limit the magnetoresistivity is only determined by the carrier density, and irrelevant to the external scatterings. Thus we dub it the intrinsic magnetoresistivity. The effect becomes measurable when the Fermi wave length is comparable with the magnetic length, i.e., the carrier density is low such that the Fermi level crosses near the Weyl nodes for the Dirac semimetals and is close to the bottom of the conduction bands for the narrow-gap semiconductors or topological insulators. In the quantum oscillatory regime, a formula for the phase shift is presented as a function of the mobility and the magnetic field, which will be useful for data analysis

Model and the Kubo-Streda formula for conductivity-To illustrate the effect of the intrinsic magnetoresistivity, we start with the Dirac Hamiltonian in a finite magnetic field, which describes either the Dirac semimetals or the narrow-gap semiconductors and topological materials,

$$\mathcal{H} = \begin{bmatrix} \Delta & v\hbar\sigma \cdot (\mathbf{k} - e\mathbf{A}) \\ v\hbar\sigma \cdot (\mathbf{k} - e\mathbf{A}) & -\Delta \end{bmatrix}. \quad (1)$$

Here v is the effective velocity and 2Δ is the energy gap between the conduction band and valence band. σ_α ($\alpha = x, y, z$) are the Pauli matrices. Without loss of generality, we assume the magnetic field is applied along the z -direction. The vector potential is then chosen as $\mathbf{A} = (-By, 0, 0)$. We focus on the situation in which the Fermi level μ is above the energy gap 2Δ . In the absence of a magnetic field, the Fermi level μ is related to the Fermi wave vector k_f , $\mu^2 = \Delta^2 + (\hbar v k_f)^2$, or the Fermi wave length $1/k_f$. In a finite field, the energy spectrum has the form, $\varepsilon_n^\zeta = \zeta \sqrt{v^2 \hbar^2 k_z^2 + 2n(\hbar v/l_B)^2} + \Delta^2$ where $l_B = \sqrt{\hbar/eB}$ is the magnetic length and $\zeta = \pm 1$ is the band index and each band is doubly degenerate in energy for $n = 1, 2, \dots$, and non-degenerate for $n = 0$, as shown in Fig.1(a).

We consider the short-range point-like impurities $U = u_0 \sum_l \delta(\mathbf{r} - \mathbf{R}_l)$ with the impurity concentration n_i . In this work, we utilize the Kubo-Streda formula[37] to calculate the

matrix element of conductivity tensor

$$\sigma_{\alpha\beta} = \frac{\hbar e^2}{2\pi V} \sum_k \int_{-\infty}^{+\infty} d\xi n_F(\xi) \text{Tr} \left[\hat{v}^\alpha \frac{dG^R}{d\xi} \hat{v}^\beta (G^A - G^R) - \hat{v}^\alpha (G^A - G^R) \hat{v}^\beta \frac{dG^A}{d\xi} \right] \quad (2)$$

here V is the volume of the system, $\hat{v}^\alpha \equiv \frac{1}{\hbar} \frac{\partial \mathcal{H}}{\partial k_\alpha}$ is the velocity operator along α -direction with $\alpha = x, y, z$, $n_F(\xi) = [1 + \exp(\frac{\xi - \mu}{k_B T})]^{-1}$ is the Fermi-Dirac distribution with k_B being the Boltzmann constant and T being the absolute temperature, $G^{R/A}(\xi) = \frac{1}{\xi - \mathcal{H} \pm i\gamma}$ are the retarded and advanced Green's functions. In the Born approximation, the scattering time $\tau = \frac{\hbar}{2\gamma} = \hbar / (2\pi N_f n_i u_0^2)$ with the density states $N_f = \mu k_f / (\pi \hbar^3 v^3)$ at the Fermi level. With the help of the eigen functions of the Landau levels, all the elements of the conductivity tensor can be expressed as the series summation over the Landau index n at the zero temperature (see Eq. [13,14,19] in the Supplementary Material [38]).

The calculated longitudinal (the electric field is parallel to the magnetic field) conductivity σ_{zz} , in-plane transverse (the electric field is perpendicular to the field) conductivity $\sigma_{xx} = \sigma_{yy}$ and the Hall conductivity σ_{xy} are plotted in Fig. 1b, which can be divided into three different regimes: (I) the semiclassical regime, (II) the quantum oscillation regime, and (III) the quantum limit regime. In the semiclassical regime, the energy band broadening width γ is larger than the energy spacing of two adjacent Landau levels near the Fermi level μ , $\gamma > (\varepsilon_{m+1}^+ - \varepsilon_m^+) / 2 \approx \hbar^2 v^2 e B / (2\hbar\mu)$ or $\chi_0 B < 1$ with the mobility $\chi_0 = e\hbar v^2 / (2\gamma\mu)$. Thus the Shubnikov-de Haas oscillations will be smeared out by disorder effect in this regime. In the quantum oscillation regime $\chi_0 B > 1$, the Landau levels near the Fermi level μ will be well separated from each other and the quantum oscillations become distinct. Further increasing the magnetic field $k_f l_B < \sqrt{2}$, all the charge carriers will be confined into the lowest Landau level, which is also named as the quantum limit.

Intrinsic magnetoresistivity-In the semiclassical regime, the longitudinal magnetoconductivity σ_{zz} is usually thought to be absent in the approximation of a spherical Fermi surface. In the weak field limit we find that $\sigma_{zz} = \sigma_0 = \frac{e^2 v^2 k_f^3}{3\pi^2 \mu} \tau$ and the electric mobility $\chi = \chi_0 = \frac{e v^2}{\mu} \tau$, which are identical to the results of the free Dirac fermions in the absence of the magnetic field. The in-plane transverse conductivity decays with increasing magnetic field due to the Lorentz force, $\sigma_{xx} = \frac{\sigma_0}{1 + (\chi_0 B)^2}$. In this case, although the transverse conductivity decays with the magnetic field, both the longitudinal and transverse magnetoresistivity are absent, $\rho_{xx} = \rho_{zz} = 1/\sigma_0$ [2]. However, a detailed calculation of the series summation of the conductivity tensor at a finite field shows a quantum correction to either the conductivity or the mobility. We perform the summation over the Landau levels with the help of the Hurwitz zeta function $\zeta(s, z) = \sum_n (n+z)^{-s}$ and the digamma function $\psi(z)$, and then utilize the asymptotic expansion of the digamma function and Hurwitz zeta func-

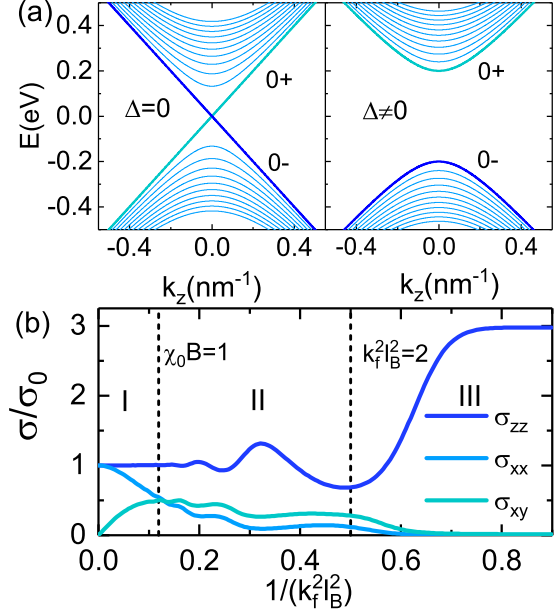


FIG. 1. (a) The band structure of Dirac fermions for the gapless case $\Delta = 0$ (the left panel) and the massive case $\Delta \neq 0$ (the right panel). (b) The conductivity as a function of a magnetic field, or magnetoconductivity of massless Dirac fermions. σ_{zz} is the longitudinal magnetoconductivity for $\mathbf{B} \parallel \mathbf{E}$ configuration, σ_{xx} is the in-plane transverse magnetoconductivity for $\mathbf{B} \perp \mathbf{E}$ configuration, and σ_{xy} is the Hall conductivity. The shown dimensionless magnetic field scales (vertical dashed lines) indicate the borders of the different regimes: (I) the semiclassical regime ($\chi_0 B < 1$) where Landau levels are smeared out due to the disorder broadening and the background dominates the magnetoconductivity; (II) quantum oscillation regime ($\chi_0 B > 1$) where Shubnikov-de Haas oscillation occurs; (III) the quantum limit regime ($k_f l_B < \sqrt{2}$), where only zero Landau level contributes.

tion for a large z , $\psi(z) = \log z - \frac{1}{2z} - \frac{1}{12z^2} + \dots$ and $\zeta(2, z) = \frac{1}{z} + \frac{1}{2z^2} + \frac{1}{6z^3} + \dots$, keeping up to the $(k_f l_B)^{-4}$ terms, to evaluate the conductivity [see Sec.S6 in Ref.[38] for the calculation].

After some cumbersome but straightforward calculation, we find that the longitudinal conductivity is expressed as $\sigma_{zz} = \sigma_0 \left[1 - \frac{c_z}{(k_f l_B)^4} \right]$ and the transverse conductivity as $\sigma_{xx} = \frac{\sigma_0}{1 + \chi^2 B^2} \left[1 - \frac{c_x}{(k_f l_B)^4} \right]$ with the mobility $\chi = \chi_0 \left[1 + \frac{c_x}{(k_f l_B)^4} \right]$. The mobility is derived from the ratio of the Hall conductivity to the transverse conductivity, $\chi = \sigma_{xy} / \sigma_{xx} B$. The quadratic correction is consistent with the Casimir-Onsager reciprocity relation $\sigma_{\alpha\alpha}(B) = \sigma_{\alpha\alpha}(-B)$ as a consequence of the time-reversal symmetry [39]. The dimensionless parameter $1/(k_f l_B)$ can be understood as the ratio of the Fermi wave length $\lambda_f = 1/k_f$ to the magnetic length l_B . The Fermi wave vector k_f is determined by the carrier density ρ , i.e., $k_f = (3\pi^2 \rho)^{1/3}$. Alternatively, $(k_f l_B)^{-2} = \frac{B}{2B_F}$ with $B_F = \frac{\hbar}{2e} k_f^2$. Comparison of these semiclassical formulae and the numerical results are shown

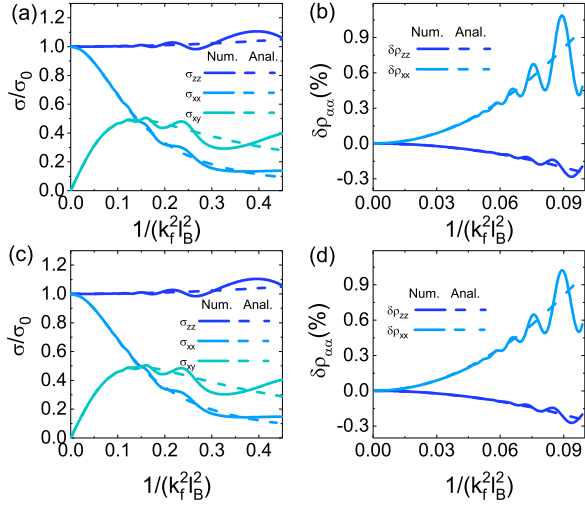


FIG. 2. (a) The magnetoconductivity and (b) magnetoresistivity for massless Dirac fermions ($\Delta = 0$). The dashed lines are the explicit numerical results and the solid lines are the corresponding analytic results in the semiclassical regime. (c) The magnetoconductivity and (d) magnetoresistivity for massless Dirac fermions ($\Delta/\hbar v k_f = 0.3$). The broadening width is $\frac{\gamma}{\hbar v k_f} = 0.07$. $k_f = 0.13 \text{nm}^{-1}$ throughout the work. The calculated coefficients are $c_x = 1$ for both the massless and massive case.

in Fig. 2a and 2c for massless and massive Dirac fermions, respectively. We find that the semiclassical formulae for conductivity are in a good agreement with the numerical results in whole semiclassical regime.

The magnetoresistivity $\rho_{\alpha\alpha}(B)$ is derived from the inverse of the conductivity tensor. Here we stress the importance of the complete set of the conductivity tensor to produce the accurate and correct behaviors of the magnetoresistivity. Denote the relative magnetoresistivity by $\delta\rho_{\alpha\alpha} = \rho_{\alpha\alpha}(B)/\rho(0) - 1$. In a weak field, the relative magnetoresistivity can be expressed as

$$\delta\rho_{\alpha\alpha}(B) = \frac{c_\alpha}{(l_B k_f)^4} = c_\alpha \left(\frac{B}{2B_F} \right)^2. \quad (3)$$

The formula is also in a good agreement with the numerical results as shown in Fig. 2b and Fig. 2d. The relative magnetoresistivity is the main result in this work.

The dimensionless coefficients c_α ($\alpha = x, y, z, \chi$) are functions of the broadening width γ and the energy gap Δ . It is noted that c_z for the longitudinal magnetoresistivity is always negative and $c_x = c_y$ for the transverse magnetoresistivity are always positive for either the massless or massive Dirac fermions. In the weak scattering limit the band broadening width $\gamma \rightarrow 0$, it is found that $c_x = 1$, $c_z = -1/4$ and $c_\chi = -3/4$, irrelevant to the external scattering [see Sec.S6 in Ref.[38] for the calculation]. In this case, the magnetoresistivity is determined by the Fermi wave vector k_f . For a specific Fermi level μ the band gap Δ can tune the Fermi wave vector via $k_f = \sqrt{\mu^2 - \Delta^2}/\hbar v$, but for a specific carrier density ρ ,

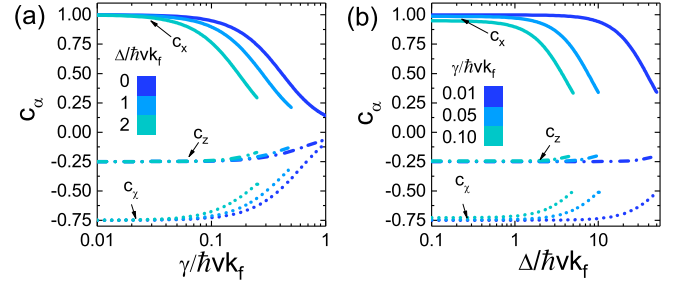


FIG. 3. The dimensionless coefficients (c_α) of the magnetoresistivities and electric mobility as a function of (a) the broadening width with different energy gap and (b) energy gap with different broadening width. All of the lines are plotted with the constraint of $\hbar^2 v^2 k_f^2 > 2\Delta\gamma$, i.e., in the semiclassical regime.

the Fermi wave vector is given by $k_f = (3\pi^2 \rho)^{1/3}$, irrelevant to the band gap. Thus the magnetoresistivity is determined by the electronic band structure and is intrinsic. A similar intrinsic magnetoconductivity was produced by the Berry curvature of the band structure in the semiclassical theory [26]. The intrinsic effect can be suppressed by the strong impurity scattering. The calculated coefficients as functions of the broadening width γ and the gap Δ as shown in Fig. 3. For a weak scattering $\gamma < 0.1\hbar v k_f$, the coefficients are rather robust against γ , but decays quickly to zero for a large γ . However for a strong disorder scattering the validity of the Born approximation is a question. For a large gap, the coefficients also decay very quickly.

Phase shift in the quantum oscillation regime-The quantum oscillation in the regime II is known as the Shubnikov-de Haas oscillation, which is described by the Lifshitz-Kosevich formula [40]. By introducing the Dingle factor $\lambda_D = \pi/(\chi_0 B)$ for the Lorentz distribution function in the series summation in the conductivity, which is a function of the mobility χ_0 and the magnetic field B , the relative oscillatory part of conductivity is approximately described by

$$\delta\rho_{\alpha\alpha}^{os} = \frac{d_\alpha}{k_f l_B \cos 2\pi\phi(B)} \text{Li}_{\frac{1}{2}} \left(e^{-\frac{\pi}{\chi_0 B}} \right) \cos \left[2\pi \left(\frac{B_F}{B} + \phi(B) \right) \right] \quad (4)$$

with the pre-factors $d_x = 7\sqrt{2}/4$ and $d_z = \sqrt{2}$. $\text{Li}_s(z)$ is the polylogarithm function of order s and argument z . ϕ_B is not a constant, but a slow-varying phase shift as a function of the Dingle factor,

$$2\pi\phi(B) = \arctan \left\{ \frac{\text{Re} \left[\sqrt{2} \exp(i\frac{3\pi}{4}) \text{Li}_{\frac{1}{2}} \left(i e^{-\frac{\pi}{\chi_0 B}} \right) \right]}{\text{Li}_{\frac{1}{2}} \left(e^{-\frac{\pi}{\chi_0 B}} \right)} \right\}. \quad (5)$$

In the quantum oscillatory regime, the field B is confined by $\chi_0 B_F > \frac{B_F}{B} > 1$, and the value of the Dingle factor is between $\pi/(\chi_0 B_F)$ and π . As a consequence, the phase shift continuously varies from almost 0 to -0.238π as shown in the Fig. 4. For a specific range of a measurable magnetic field B , the value of $\phi(B)$ is mainly determined by the mobility. In

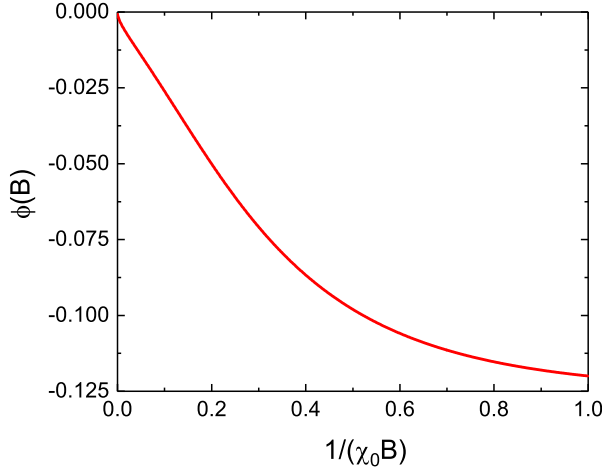


FIG. 4. The phase shift ϕ_B as a function of $1/(\chi_0 B)$.

the massless case, $\Delta = 0$, usually the mobility can be very large and the factor $\pi/\chi_0 B_F = 4\pi\gamma/(v\hbar k_f)$ is quite small, and the phase shift almost equal to zero for B has the same or less order of B_F . However for a large gap $\Delta/v\hbar k_f \gg 1$, $\pi/\chi_0 B_F = 4\pi\gamma\Delta/(v\hbar k_f)^2$ and the phase shift is close to $-\pi/4$. In practice, $\phi(B)$ and B_F can be obtained from the Landau level fan diagram. The phase shift $\phi(B)$ can be determined by the interpolation line of n versus $1/B$ (see Fig.1 in Ref. [38]). It is noted that the phase shift is only a function of the Dingle factor no matter whether the Dirac fermions are gapless or not.

Magnetoconductivity in the quantum limit-When the magnetic field grows sufficient large ($k_f \ell_B \ll 1$), only the Landau level of $n = 0$ is partially filled, i.e., the system is in the quantum limit regime [41]. So we only need to consider the $n = 0$ term in Eq.(S13) and Eq.(S14) in Ref. [38]. In the case the chemical potential varies with the magnetic field as $\mu = \sqrt{(2\pi^2 l_B^2 \hbar v \rho)^2 + \Delta^2}$ and the scattering time is evaluated as $\tau = \frac{2\pi^3 \ell_B^4 \hbar^3 v^2 \rho}{n_i u_0^2 \sqrt{(2\pi^2 l_B^2 \hbar v \rho)^2 + \Delta^2}}$ in the Born approximation. The longitudinal and transverse conductivity satisfy a relation approximately,

$$\sigma_{xx} \sigma_{zz} \simeq \frac{1}{2\pi^2 l_B^2} \left(\frac{e^2}{h} \right)^2. \quad (6)$$

The longitudinal conductivity is $\sigma_{zz} = \frac{e^2 v^2 \rho \tau}{\mu}$. For the massless case of $\Delta = 0$, $\tau = \frac{\pi \ell_B^2 \hbar^2 v}{n_i u_0^2}$ and $\mu = 2\pi^2 l_B^2 \hbar v \rho$. The resulting conductivity $\sigma_{zz} = \frac{e^2 \hbar}{2\pi} \frac{v^2}{n_i u_0^2} = \text{constant}$ and $\sigma_{xx} \propto B$ which is consistent with the results for massless Dirac fermions in Ref.[42–44]. For the large massive case of $\Delta \gg 2\pi^2 l_B^2 \hbar v \rho$, $\tau = \frac{\pi \ell_B^2 \hbar^2 v}{n_i u_0^2 \Delta}$ and $\mu \simeq \Delta$. The conductivity $\sigma_{zz} \approx \frac{2\pi^3 e^2 \hbar^3 v^4 l_B^4 \rho^2}{n_i u_0^2 \Delta^2} \propto \frac{1}{B^2}$, which indicates a negative magnetoconductivity or positive magnetoresistivity $\rho_{zz} \propto B^2$ in the longitudinal configuration. This result is consistent with the results for electron gas in semiconductor

with low carrier density[24]. Following from Eq. (6), the corresponding transverse magnetoconductivity is found to be $\sigma_{xx} \propto B^3$.

Discussions-The negative longitudinal and positive in-plane transverse magnetoresistivity reflect the anisotropic magneto-transport in the Dirac materials. The difference of the two resistivities $\rho_{zz} - \rho_{xx} = \frac{c_z - c_x}{\sigma_0} \frac{B^2}{(2B_F)^2}$ leads to a general relation between the electric field \mathbf{E} and charge current density \mathbf{j} ,

$$\mathbf{E} = \rho_{\perp} \mathbf{j} + \frac{c_z - c_x}{\sigma_0} \frac{(\mathbf{j} \cdot \mathbf{B}) \mathbf{B}}{(2B_F)^2} + \rho_{\perp} \chi \mathbf{B} \times \mathbf{j}. \quad (7)$$

with $\rho_{\perp} = \frac{1}{\sigma_0} \left(1 + c_x \frac{B^2}{(2B_F)^2} \right)$. In the x-z plane constructed by \mathbf{B} and \mathbf{j} , it follows that the resistivity $\rho_{ij} = \rho_{\perp} \delta_{ij} + \frac{c_z - c_x}{\sigma_0} \frac{B_i B_j}{(2B_F)^2}$. The diagonal resistivity is anisotropic as a function of the angle φ between the magnetic field and electric current density, i.e., anisotropic magnetoresistivity (AMR), $\rho_{zz} = \frac{1}{\sigma_0} \left(1 + \frac{c_z + c_x}{2} \frac{B^2}{(2B_F)^2} + \frac{c_z - c_x}{2} \frac{B^2}{(2B_F)^2} \cos 2\varphi \right)$, and the off-diagonal AMR or planar Hall resistivity is $\rho_{xz} = \frac{c_z - c_x}{2\sigma_0} \frac{B^2}{(2B_F)^2} \sin 2\varphi$. This planar Hall resistivity satisfies the symmetric relation, $\rho_{xz} = \rho_{zx}$, unlike the ordinary Hall resistivity which is perpendicular to the magnetic field, and has an anti-symmetric relation. The oscillatory amplitude is quadratic in the field B . This effect was recently discussed and explored in the Dirac semimetals [45–49].

The effect becomes strong when the carrier density is low and the electric mobility is high. The characteristic field for this intrinsic magnetoresistivity is one magnetic quantum flux $\phi_0 = h/2e$ per Fermi wave length area $\pi \lambda_f^2$. For a density $\rho = \rho_0 \times 10^{16}/\text{cm}^3$, the field is about $2B_F \approx 2.92 \rho_0^{2/3} \text{T}$. It increases two orders if the density changes three orders. For $\rho_0 = 10^3$, $2B_F \approx 292 \text{T}$. To have an observable magnetoresistivity, the carrier density should be lower than $\rho = 10^{19}/\text{cm}^3$. In fact it has been observed that the magnetoresistance in n-doped germanium is enhanced with lowering the concentration of impurity [50], which is possibly related to the present intrinsic mechanism of magnetoresistance. Recent discovered Weyl and Dirac semimetals [3] may provides samples with low carrier density and high mobility as the Fermi level is expected to cross near the Weyl nodes, which are good candidates for measuring the intrinsic effect.

Finally it is worthy of pointing out that the origin of the intrinsic negative magnetoresistivity is apparently different from that from chiral anomaly of Weyl fermions. The chiral anomaly occurs for massless Weyl fermions in the presence of both electric and magnetic field, and should be absent for massive fermions. The intrinsic negative magnetoresistivity persists for either massless or massive Dirac fermions. Meanwhile the large positive transverse magnetoresistivity is also irrelevant with the mechanism of chiral anomaly as the electric field is perpendicular to the magnetic field.

This work was supported by the Research Grants Council, University Grants Committee, Hong Kong under Grant No.

17301116 and C6026-16W.

H.W.W. and B.F. contributed equally to this work.

* sshen@hku.hk

- [1] A. A. Abrikosov, *Fundamentals of the Theory of Metals* (North-Holland, Amsterdam, 1988).
- [2] A. B. Pippard, *Magnetoresistance in metals*, vol. 2 (Cambridge University Press, Cambridge, 1989).
- [3] N. Armitage, E. Mele, and A. Vishwanath, *Rev. Mod. Phys.* **90**, 015001 (2018).
- [4] H. Z. Lu and S. Q. Shen, *Front. Phys.* **12**, 127201 (2017).
- [5] H. J. Kim, K. S. Kim, J. F. Wang, M. Sasaki, N. Satoh, A. Ohnishi, M. Kitaura, M. Yang, and L. Li, *Phys. Rev. Lett.* **111**, 246603 (2013).
- [6] J. Xiong, S. K. Kushwaha, T. Liang, J. W. Krizan, M. Hirschberger, W. Wang, R. Cava, and N. Ong, *Science* **350**, 413 (2015).
- [7] Q. Li, D. E. Kharzeev, C. Zhang, Y. Huang, I. Pletikoscic, A. V. Fedorov, R. D. Zhong, J. A. Schneeloch, G. D. Gu, and T. Valla, *Nat. Phys.* **12**, 550 (2016).
- [8] C. Z. Li, L. X. Wang, H. Liu, J. Wang, Z. M. Liao, and D. P. Yu, *Nat. Commun.* **6**, 10137 (2015).
- [9] H. Li, H. He, H. Z. Lu, H. Zhang, H. Liu, R. Ma, Z. Fan, S. Q. Shen, and J. Wang, *Nat. Commun.* **7**, 10301 (2016).
- [10] X. Huang, L. Zhao, Y. Long, P. Wang, D. Chen, Z. Yang, H. Liang, M. Xue, H. Weng, Z. Fang, et al., *Phys. Rev. X* **5**, 031023 (2015).
- [11] C. L. Zhang, S. Y. Xu, I. Belopolski, Z. Yuan, Z. Lin, B. Tong, G. Bian, N. Alidoust, C. C. Lee, S. M. Huang, et al., *Nat. Commun.* **7**, 10735 (2016).
- [12] Z. Wang, Y. Zheng, Z. Shen, Y. Lu, H. Fang, F. Sheng, Y. Zhou, X. Yang, Y. Li, C. Feng, et al., *Phys. Rev. B* **93**, 121112 (2016).
- [13] C. Zhang, E. Zhang, W. Wang, Y. Liu, Z. G. Chen, S. Lu, S. Liang, J. Cao, X. Yuan, L. Tang, et al., *Nat. Commun.* **8**, 13741 (2017).
- [14] J. Wang, H. Li, C. Chang, K. He, J. S. Lee, H. Lu, Y. Sun, X. Ma, N. Samarth, S. Shen, et al., *Nano Res.* **5**, 739 (2012).
- [15] H. He, H. Liu, B. Li, X. Guo, Z. Xu, M. Xie, and J. Wang, *Appl. Phys. Lett.* **103**, 031606 (2013).
- [16] S. Wiedmann, A. Jost, B. Fauque, J. van Dijk, M. Mei-er, T. Khouri, S. Pezzini, S. Grauer, S. Schreyeck, C. Brune, et al., *Phys. Rev. B* **94**, 081302 (2016).
- [17] B. Assaf, T. Phuphachong, E. Kampert, V. Volobuev, P. Mandal, J. Sanchez-Barriga, O. Rader, G. Bauer, G. Springholz, L. de Vaulchier, et al., *Phys. Rev. Lett.* **119**, 106602 (2017).
- [18] S. L. Adler, *Phys. Rev.* **177**, 2426 (1969).
- [19] J. S. Bell and R. Jackiw, *Il Nuovo Cimento A* **60**, 47 (1969).
- [20] H. B. Nielsen and M. Ninomiya, *Phys. Lett. B* **130**, 389 (1983).
- [21] D. T. Son and B. Z. Spivak, *Phys. Rev. B* **88**, 104412 (2013).
- [22] A. A. Burkov, *Phys. Rev. Lett.* **113**, 247203 (2014).
- [23] A. A. Burkov, *J. Phys. Condens. Matter* **27**, 113201 (2015).
- [24] P. Goswami, J. H. Pixley, and S. Das Sarma, *Phys. Rev. B* **92**, 075205 (2015).
- [25] E. V. Gorbar, V. A. Miransky, and I. A. Shovkovy, *Phys. Rev. B* **89**, 085126 (2014).
- [26] Y. Gao, S. A. Yang, and Q. Niu, *Phys. Rev. B* **95**, 165135 (2017).
- [27] A. V. Andreev and B. Z. Spivak, *Phys. Rev. Lett.* **120**, 026601 (2018).
- [28] S. Murakami, *New J. Phys.* **9**, 356 (2007).
- [29] A. A. Burkov, *Nat. Mater.* **15**, 1145 (2016).
- [30] B. Yan and C. Felser, *Annu. Rev. Condens. Matter Phys.* **8**, 337 (2017).
- [31] E. O. Kane, *J. Phys. Chem. Solids* **1**, 249 (1957).
- [32] S. Q. Shen, *Topological insulators* (Springer Nature, Singapore, 2017), 2nd ed.
- [33] S. Q. Shen, W. Y. Shan, and H. Z. Lu, *SPIN* **01**, 33 (2011).
- [34] W. Zawadzki, *J. Phys. Condens. Matter* **29**, 373004 (2017).
- [35] M. C. Chang and Q. Niu, *J. Phys. Condens. Matter* **20**, 193202 (2008).
- [36] D. Xiao, M. C. Chang, and Q. Niu, *Rev. Mod. Phys.* **82**, 1959 (2010).
- [37] P. Streda, *J. Phys. C: Solid State Phys.* **15**, L1299 (1982).
- [38] See Supplemental Material for the calculation details, which includes Refs. [25, 37, 40, 44, 51–56]
- [39] L. Onsager, *Phys. Rev.* **37**, 405 (1931).
- [40] D. Shoenberg, *Magnetic Oscillations in Metals* (Cambridge University Press, Cambridge, 1984).
- [41] A. A. Abrikosov, *Phys. Rev. B* **58**, 2788 (1998).
- [42] H. Z. Lu, S. B. Zhang, and S. Q. Shen, *Phys. Rev. B* **92**, 045203 (2015).
- [43] S. B. Zhang, H. Z. Lu, and S. Q. Shen, *New J. Phys.* **18**, 053039 (2016).
- [44] J. Klier, I. V. Gornyi, and A. D. Mirlin, *Phys. Rev. B* **96**, 214209 (2017).
- [45] A. A. Burkov, *Phys. Rev. B* **96**, 041110 (2017).
- [46] S. Nandy, G. Sharma, A. Taraphder, and S. Tewari, *Phys. Rev. Lett.* **119**, 176804 (2017).
- [47] H. Li, H.W. Wang, H. He, J. Wang, and S. Q. Shen, arXiv:1711.03671 (2017).
- [48] M. Wu, G. Zheng, W. Chu, W. Gao, H. Zhang, J. Lu, Y. Han, J. Yang, H. Du, W. Ning, et al., arXiv:1710.01855 (2017).
- [49] N. Kumar, C. Felser, and C. Shekhar, arXiv:1711.04133 (2017).
- [50] M. Glicksman, *Phys. Rev.* **108**, 264 (1957).
- [51] S. Q. Shen, Y. J. Bao, M. Ma, X. C. Xie, and F. C. Zhang, *Phys. Rev. B* **71**, 155316 (2005).
- [52] W. Magnus and F. Oberhettinger, *Formeln und Satze fur die Speziellen Funktionen der Mathematischen Physik* (Springer, Berlin, 1943).
- [53] B. Fu, W. Zhu, Q. Shi, Q. Li, J. Yang, and Z. Zhang, *Phys. Rev. Lett.* **118**, 146401 (2017).
- [54] E. Elizalde, S. D. Odintsov, A. Romeo, A. A. Bytsenko, and S. Zerbini, *Zeta regularization techniques with applications* (World Scientific, Singapore, 1994).
- [55] A. Bastin, C. Lewiner, O. Betbeder-Matibet, and P. Nozieres, *J. Phys. Chem. Solids* **32**, 1811 (1971).
- [56] C. M. Wang, H. Z. Lu, and S. Q. Shen, *Phys. Rev. Lett.* **117**, 077201 (2016).